

# Analysis of corneal morphologic and pathologic changes in early-stage congenital aniridic keratopathy

Juan Du<sup>1</sup>, Rong-Qiang Liu<sup>2,3</sup>, Lei Ye<sup>2</sup>, Zhi-Hui Li<sup>1</sup>, Feng-Tu Zhao<sup>1</sup>, Nan Jiang<sup>2</sup>, Lin-Hong Ye<sup>2</sup>, Yi Shao<sup>2</sup>

<sup>1</sup>Department of Ophthalmology, the First People's Hospital of Shunde, Nanfang Medical University, Foshan 528300, Guangdong Province, China

<sup>2</sup>Department of ophthalmology, the First Affiliated Hospital of Nanchang University, Jiangxi Province Clinical Ophthalmology Institute, Nanchang 330006, Jiangxi Province, China

<sup>3</sup>Postgraduate College, the Third hospital Affiliated of Sun Yat-sen University, Guangzhou 510000, Guangdong Province, China

**Co-first authors:** Juan Du and Rong-Qiang Liu

**Correspondence to:** Yi Shao. Department of Ophthalmology, the First Affiliated Hospital of Nanchang University, Nanchang 330006, Jiangxi Province, China. Freebee99@163.com

Received: 2016-04-16 Accepted: 2016-07-06

## Abstract

• **AIM:** To determine typical corneal changes of congenital aniridic keratopathy (CAK) using corneal topography and confocal systems, and to identify characteristics that might assist in early diagnosis.

• **METHODS:** Patients with CAK and healthy control subjects underwent detailed ophthalmic examinations including axial length, corneal thickness, tear film condition, corneal topography, and laser-scanning *in vivo* confocal microscopy (IVCM).

• **RESULTS:** In early stage aniridic keratopathy, Schirmer I test (SIT), break-up time (BUT), mean keratometry (mean K) and simulated keratometry (sim K) were reduced relative to controls ( $P < 0.05$ ), while simulation of corneal astigmatism (sim A) and corneal thickness were increased ( $P < 0.05$ ). In addition, significantly more eyes exhibited flat cornea compared with the control group. Inflammatory dendritic cells were present in the aniridic epithelium, with significantly increased density relative to controls ( $P < 0.05$ ). Palisade ridge-like features and abnormal cell morphology were observed in six out of sixteen CAK cases. In central cornea area, the aniridic corneas had the increased subbasal nerve density.

• **CONCLUSION:** These changes in corneal morphology in borderline situations can be useful to confirm the diagnosis of CAK.

• **KEYWORDS:** aniridic keratopathy; corneal topography; confocal microscopy

**DOI:**10.18240/ijo.2017.03.09

Du J, Liu RQ, Ye L, Li ZH, Zhao FT, Jiang N, Ye LH, Shao Y. Analysis of corneal morphologic and pathologic changes in early-stage congenital aniridic keratopathy. *Int J Ophthalmol* 2017;10(3):378-384

## INTRODUCTION

Aniridia is a rare congenital disorder that is characterized by varying degrees of hypoplasia of the iris. The prevalence and incidence are between one over fifty thousand and one over one hundred thousand, respectively. Based on geographic differences, two-thirds of patients have a family history of the disorder. The remaining patients coincide with sporadic diseases, including some cases of WAGR (Wilms tumour, Aniridia, Genitourinary anomalies and Retardation) syndrome caused by the deletion of chromosome region 11q13. Up to 60% of sporadic disease is in fact inherited, and such patients often have concomitant conditions such as intellectual disabilities or Wilms tumors<sup>[1-3]</sup>.

Congenital aniridic keratopathy (CAK) has diverse clinical manifestations and enormous phenotypic variations, even among patients in the same family. The most obvious clinical symptoms are dysplasia of the iris and the presence of other diseases associated with early pathologic progression in the eye, such as congenital or infantile glaucoma and Rieger syndrome<sup>[4-6]</sup>. In early stages of the disease, patients suffer from blurred vision; with age, vision decreases significantly. CAK can also cause corneal opacity and glaucoma, which often impact both vision and quality of life<sup>[7]</sup>. The diagnosis of CAK depends on recognizing its clinical manifestations. Furthermore, early detection and treatment are key to reducing complications.

The majority of research into CAK has concentrated on the lens and retina, while pathologic changes to the cornea are less well understood. The aims of the present study were to determine the typical corneal changes of CAK using corneal topography and confocal systems, and to identify characteristics that might assist in early diagnosis.

## SUBJECTS AND METHODS

**Study Population** This prospective case-control study recruited patients with CAK who attended the Ophthalmology Department of the First Affiliated Hospital of Nanchang University (Nanchang, Jiangxi Province, China) between October 2009 and June 2014.

A total of 80 aniridia patients were traced and recorded. Totally 16 subjects were recruited for the present study, based on a

practical limitation of those residing in regions surrounding academic hospitals where full examinations could be conducted. The control group recruited during conventional medical examinations, comprised healthy age- and sex-matched volunteers with an uncorrected visual acuity score  $>1.0$ , no history of trauma, no contact lens use, no refractive surgery, and normal eye development. The axial length and corneal thickness of patients and volunteers were measured, and tear film, corneal topography, and corneal confocal scanning were conducted. The study was authorized by the Ethics Committee of the First Affiliated Hospital of Nanchang University. For each subject, the study protocol and procedure were fully explained, and consent was obtained. All methods of this research followed the Declaration of Helsinki and conformed to the principles of medical ethics.

Exclusion criteria were: the presence of factors that might introduce refractive errors (*e.g.* keratoconus, corneal laser surgery, trauma); a history of contact lens use; and the presence of familial keratoconus, chronic keratitis or conjunctivitis, atopic disease, or other systemic diseases. Patients with secondary glaucoma were required to maintain normal intraocular pressure (IOP) and to have a transparent cornea (determined using a corneal endothelial mirror), a normal ratio of hexagonal cells to corneal endothelial cells, and normal cell densities.

**Axial Length and Corneal Thickness** Ocular axial length was measured using A-mode ultrasonic diagnostic equipment, with the mean of five repeated measurements used for analysis. Measurement of axial length was conducted using A/B-SCAN-CINESCAN (Quantel Medical, France).

We applied dopey cornea after the probe light in the corneal vertex and recorded the peak and stable values, selecting the distance between the first and last waves as the axial length. This was repeated five times for each participant.

#### **Corneal Topography and Corneal Confocal Microscopy**

The Pentacam (Oculus, Germany) was used for corneal topography, and *in vivo* confocal microscopy (IVCM; HRT3-RCM, Heidelberg Engineering, Germany) was used to evaluate cellular changes in the cornea, including quantification of subbasal nerve density and Langerhans/dendritic cell density in the central cornea. With the participant seated, the lower jaw was lifted and the head was restrained with the eyes looking at the front lamp. The eyes were kept open with a light focusing at the center of the pupil for 2s, and corneal images were exported to a computer system. Images included a color-code chart, anterior and posterior corneal surface-elevation maps, a corneal surface-gravity map, and refractive corneal thickness figures. A total of nine corneal regions (central, superotemporal, temporal, inferotemporal, inferior, inferonasal, nasal, superonasal, superior) were identified, analyzed, and documented. Study parameters included central thinnest corneal depth, degree of corneal astigmatism (mean A),

simulation of corneal astigmatism (sim A), mean keratometry (mean K), simulated keratometry (sim K), irregularity in the 3 mm zone, irregularity in the 5 mm zone, and the mean thickness of nine distinct corneal regions (2 mm diameter circles, 3 mm from the optical axis; one at the central cornea and eight in the periphery). Corneal topography was classified based on anterior corneal surface refraction (*i.e.* round, oval, symmetrical bowknot, asymmetric bowknot, and irregular), corneal surface-elevation maps (*i.e.* symmetrical crest, asymmetric ridge, incomplete crest, island, and unclassified) and corneal thickness maps (*i.e.* circular, oval, eccentric circular, and eccentric oval).

Each eye was examined three times and the best corneal topography images were analyzed. When the image of the central cornea was unclear due to dry eye, eye movement, poor eye fixation, or blinking, the examination was repeated until a clear image was obtained. Binocular images were used for statistical analyses.

IVCM images were coded to blind examiners to the participant's status (*i.e.* CAK or healthy control). For dendritic cell density, only mature dendritic cells, consisting of cell bodies and processes, were counted to provide an indication of the presence of antigen-presenting cells involved in inflammation. For quantification, clear and high-contrast images of the central subbasal nerve plexus with the greatest number of visible nerves and the greatest number of visible dendritic cells were selected for each participant. These images were used to assess subbasal nerve density and mature dendritic cell density, respectively. Nerve tracing and cell counting were performed with the ImageJ software, as described previously<sup>[8]</sup>. Density values were determined by two independent trained observers, and the mean value between observers was reported. The inferior limbal region was also examined by IVCM to assess morphology in the region of the limbal Palisades of Vogt.

**Tear Film Test with Four Terms** In the process of corneal fluorescein staining, the fluorescent (FL) strips were inserted into the fornix conjunctivae inferior of each patients, followed by blinking. Then, we used a 0 to 12 point scale to record staining. We divided the cornea into four quadrants, and scored 0-3 points based on the level and proportion of each quadrant staining. According to the National Ophthalmology Research Clinical Dry Eye Score, The ratings were classified into four levels<sup>[9]</sup>: 0: no staining; 1: few disseminated stains; 2: moderate stains (between class 1 and class 3); and 3: severely fused stains. The height of the tear meniscus in the central lower eyelid was measured by a ruler under a slit-lamp microscope. Tear stability was assessed by performing a tear film break-up time (TFBUT) evaluation, which calculated the time interval between a blink and the appearance of a break in the tear film. A fluorescein strip was placed in the fornix of the lower eyelid and then removed. The patient was instructed to blink three

## Corneal changes in congenital aniridic keratopathy

times and then to look straight ahead without blinking. The tear film was observed under a slit-lamp microscope with acobalt-blue filter. Each eye was measured in triplicates, and the average of each eye was selected for further analysis. Schirmer I test (SIT): a thin strip of filter paper (35×5 mm) was applied for quantify tear production over a period of 5min. The strip was placed at the junction of the moderate and lateral thirds of the lower eyelid. All patients look forward and blink normally according instruction during the test.

**Statistical Analysis** Measurement data were presented as mean±SD (range) and were compared using *t*-test between groups. Ranked data with a median (range) were compared between groups using the Wilcoxon test and rates were compared by Chi-square test between groups. All statistical analyses were performed using SPSS version 19.0 (SPSS Inc., Chicago, IL, USA) for Windows. *P* values <0.05 were considered statistically significant.

## RESULTS

The study recruited 16 patients with CAK (6 males/10 females; mean age 10±4y; age range 7-14y) and 16 control subjects (7 males/9 females; mean age 11±3y; age range 6-14y). There were no statistically significant between-group differences in age or gender (*P*>0.05 for each comparison). The average axial length (mm) was 24.06±2.74 and the average corneal diameter (mm) was 10.28±1.96 in the patient group. In contrast, in the control, the average axial length (mm) was 24.66±2.19 and the average corneal diameter (mm) was 11.86±1.52. There were statistically significant between-group differences in corneal diameter (*P*<0.05).

Data regarding tear films characteristics are shown in Table 1. Patients with CAK had significantly lower SIT, break-up time (BUT) and height of tear meniscus (HTM) and significantly higher FL scores than control subjects (*P*<0.05 for each comparison; Table 1).

Corneal topography data are shown in Table 2. Patients with CAK had significantly lower mean K and sim K than those in the control group (*P*<0.05 for each comparison; Table 2). Patients with CAK had significantly greater sim A, 3.0 mm irregularity and 5.0 mm irregularity than those in the control group (*P*<0.05 for each comparison; Table 2). There was no significant difference for mean A in both groups (*P*>0.05).

In addition, significantly more eyes in the patient group exhibited flat cornea compared with the control group (*P*<0.05; Table 2). There was a significant between-group difference in the morphology of the anterior corneal surface (*P*<0.05; Table 2). The central curvature of the cornea was significantly lower in patients than controls (*P*<0.05; Table 2).

The thinnest part of the cornea was detected in the middle cornea in both groups. The thickness of the thinnest cornea (µm) was 596±36 in the patient group, whereas that of the control group was 532±25 µm. In terms of the thickness of

**Table 1 Tear film characteristics in patients with CAK and healthy control subjects** (n=16 subjects with 32 eyes per group)

Parameters	CAK group	Control group	<i>t</i> / <i>Z</i>	<i>P</i>
SIT	13.86±3.68 <sup>a</sup>	20.36±5.22	8.742	0.035
BUT	8.38±2.96 <sup>a</sup>	16.92±4.28	6.195	0.012
FL	1.22±0.98 <sup>a</sup>	1.06±1.01	7.242	0.039
HTM	0.42±0.16 <sup>a</sup>	0.72±0.22	9.925	0.017
IOP	18.64± 3.82	15.42±2.67	7.249	0.029

SIT: Schirmer I test; BUT: Break-up time; FL: Fluorescent; HTM: Height of tear meniscus; IOP: Intraocular pressure. <sup>a</sup>*P*<0.05 vs control.

**Table 2 Corneal topography parameters in patients with CAK and healthy control subjects** (n=16 subjects with 32 eyes per group)

Parameters	CAK group	Control group	<i>t</i> / <i>χ</i> <sup>2</sup>	<i>P</i>
Keratometry <sup>b</sup> (D)				
Mean	41.4±1.5 (38.1-44.2) <sup>a</sup>	43.3±1.9(40.9-45.9)	18.616	0.0022
Simulated	40.6±1.2 (37.6-43.4) <sup>a</sup>	42.8±1.5 (40.3-45.1)	20.421	0.0016
Astigmatism <sup>b</sup> (D)				
Mean	1.04±0.74 (0.6-4.2)	0.96±0.29 (0.2-2.4)	1.921	0.76
Simulated	1.14±0.79 (0.5-4.5) <sup>a</sup>	0.88±0.22 (0.3-2.1)	10.853	0.009
Irregularity				
3.0 mm zone	1.66±0.92 (0.8-2.9) <sup>a</sup>	1.48±0.78 (0.5-2.0)	17.827	0.031
5.0 mm zone	1.68±1.01 (1.2-2.6) <sup>a</sup>	0.94±0.70 (0.3-1.9)	14.652	0.012
Flat cornea <sup>c</sup>	16 (66.7) <sup>a</sup>	3 (12.5)	9.495	0.002

D: Dioptre. <sup>a</sup>*P*<0.05 vs control; <sup>b</sup>Data from 3 mm zone; <sup>c</sup><41.50 D.

**Table 3 Corneal thickness in patients with CAK and healthy control subjects** (n=16 subjects with 32 eyes per group, µm)

Corneal region	CAK group	Control group	<i>t</i>	<i>P</i>
Central	636±36 <sup>a</sup>	544±29	17.317	0.008
Superotemporal	662±35 <sup>a</sup>	602±27	9.942	0.019
Temporal	682±36 <sup>a</sup>	592±30	12.637	0.015
Inferotemporal	675±29 <sup>a</sup>	587±32	25.602	0.011
Inferior	664±32 <sup>a</sup>	606±39	18.391	0.023
Inferonasal	697±42 <sup>a</sup>	634±34	9.364	0.035
Nasal	689±39 <sup>a</sup>	629±29	16.528	0.029
Superonasal	654±31 <sup>a</sup>	641±37	12.267	0.041
Superior	650±28 <sup>a</sup>	643±35	17.841	0.047

<sup>a</sup>*P*<0.05 vs control.

central cornea, 14 eyes (46.7%) were thicker than 550 µm in the patient group, while 5 eyes (16.7%) in the control. There were significant differences for the thickness of central cornea in both groups (all *P*<0.05). Data regarding corneal thickness are given in Table 3. In the patient group, the cornea was significantly thicker in the central and all other locations compared with the control group (*P*<0.05; Table 3).

The front surface of the corneal refractive and corneal thickness graph at the same age (10 years old) of normal females (Figure 1A, 1B) and congenital aniridia male patients (Figure 1C, 1D).

**In Vivo Confocal Microscopy** In three of the 16 patients with CAK, it was not possible to obtain useful IVCM images of the cornea because of severe bilateral nystagmus. In the

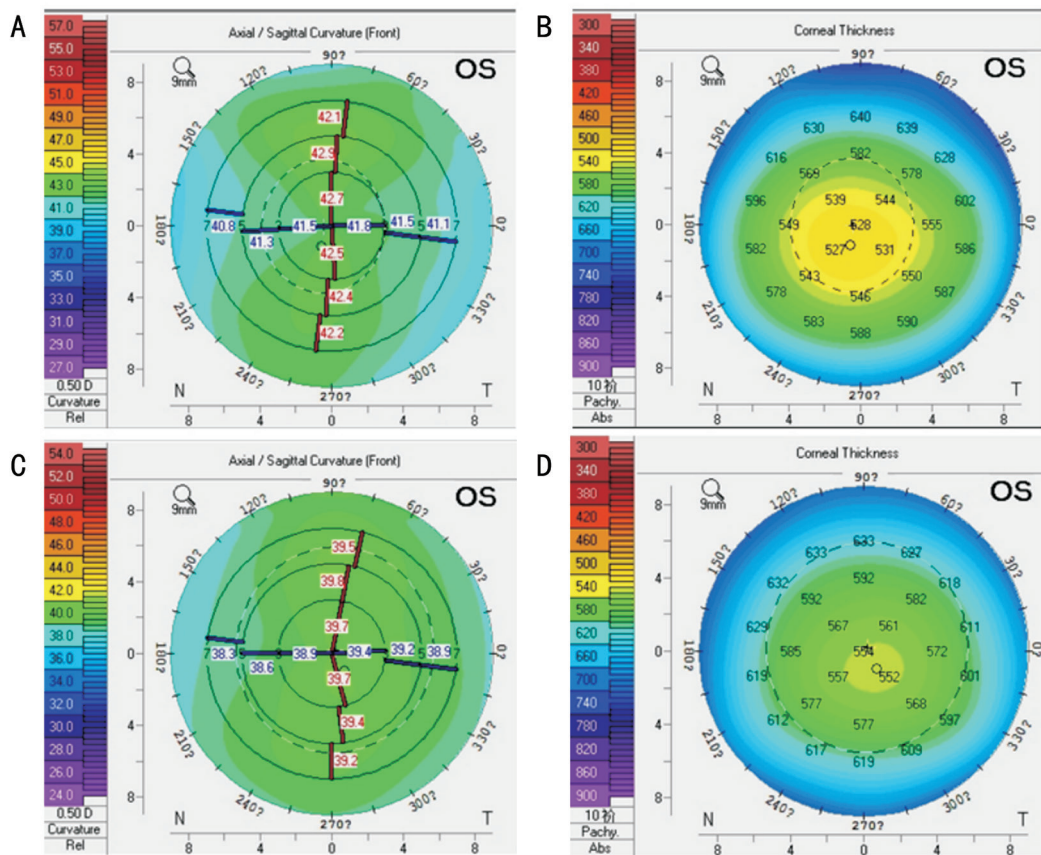


**Figure 1** The front surface of the corneal refractive and corneal thickness graph at the same age (10 years old) of normal females (A, B) and congenital aniridia male patients (C, D) A: Map of a normal patient's anterior corneal surface, the radius of the corneal curvature gradually increased from the centre to the periphery, and the shape of the cornea was oval; B: Corneal thickness graph of the nine regions in the normal group, the thinnest area of corneal depth was located in the central area of the cornea (527 mm) with an eccentric large oval; C: Map of congenital aniridia patients' anterior corneal surface, the central cornea was flat and peripheral areas exhibited greater flat, the shape of the cornea was eccentric circular; D: A corneal thickness graph of the nine regions in the congenital aniridia group, the central thickness was near normal (552 mm) and the peripheral cornea was significantly thicker with small eccentric oval morphology.

central cornea, epithelial wing cell layers of all CAK patients examined contained small, hyper-reflective inclusions indicative of inflammatory (presumably dendritic) cells (Figure 2E), while these inclusions were absent in healthy controls (Figure 2A). The density of mature dendritic cells was, however, significantly greater in patients than controls (median 78 versus 52 cells/mm<sup>2</sup>,  $P < 0.05$ ; Figure 2B, 2F). Mature dendritic cells were present in the central subbasal nerve plexus in all of the CAK patients examined and in five of 16 controls (Figure 2C, 2G). Imaging of the limbal palisades region was possible in only eight of the healthy controls, due to varying participant tolerance of the imaging procedure. In these corneas, the palisade ridges and focal stromal projections were observed. CAK corneas, however, had a distinct limbal palisades region with abnormal cell morphology. In contrast, palisade ridge-like features were observed in six patients with CAK (Figure 2D, 2H), although these features appeared to be abnormally developed.

## DISCUSSION

We previously reported the corneal morphologic changes in pure microphthalmia and Marfan syndrome<sup>[10-11]</sup>. In this study, we investigated the clinical and morphologic corneal findings

in patients in the early stages of CAK, which still maintained transparent cornea. The pathogenesis of CAK involves paired box 6 (*PAX6*) mutations that lead to abnormal development of the nerve ectoderm and mesoderm. CAK is often associated with other systemic abnormalities, such as WAGR syndrome and reduced lysis ability of red blood cells<sup>[12-13]</sup>. A large study on CAK families in China revealed that CAK patients might also be prone to glucose intolerance and even diabetes, as well as abnormal brain structures. Overall, CAK appears to be a syndrome comprising of disorders in various body systems, such as the eyes and nose<sup>[14]</sup>. *PAX6*, located on 11q13, is a candidate gene for CAK. Its haploinsufficient mutation causes disease, in which proteins translated from a single copy of a normal gene are incapable of ensuring normal function, leading to a reduction in functional *PAX6* protein<sup>[13-14]</sup>. During eye development, the *PAX6* gene plays a major role in controlling eye development<sup>[15-16]</sup> and is expressed in the edge of the optic cup and the surface ectoderm<sup>[19]</sup>.

Small corneas usually become noticeable in CAK patients before the age of 10y; other early symptoms include peripheral corneal opacity with radial pannus; shallow and irregular thickening of the corneal epithelium; positive fluorescein

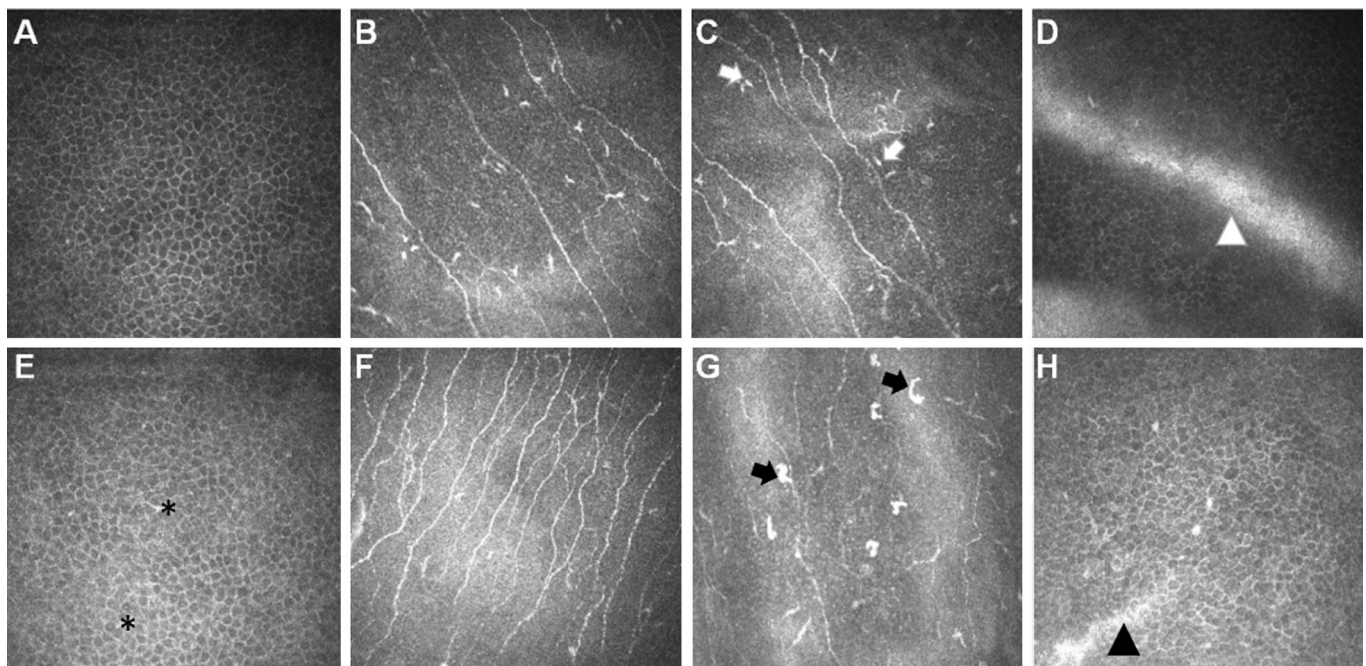


**Figure 2** *In vivo* images of the cornea in healthy controls (A-D) and in aniridia (E-H) *In vivo* appearance of epithelial wing cell morphology in the central cornea in aniridia (E) and in healthy controls (A). Small, reflective inclusions (black asterisks) indicate inflammatory dendritic cell presence in the aniridic epithelium, where these inclusions are absent in the control group. In central cornea area, the aniridic corneas (F) have higher subbasal nerve density than the control cornea (B). The majority of aniridia cases had a pathologically high density of mature dendritic cells in the central cornea at the level of the basal epithelium, while the majority of healthy controls had a normal dendritic cell density. *In vivo* images depict mature dendritic cells (black arrows) in the central cornea in aniridia (G), and mainly immature dendritic cells (cell bodies without long processes, white arrows) in the central corneas of controls (C). In the inferior limbal, the palisades region in healthy controls (D, white arrowheads) and the abnormal ridge-like features in aniridia (H, black arrowheads).

staining; and the absence of the Vogt fence<sup>[20-21]</sup>. In addition, the densities of corneal edge cells and conjunctival goblet cells are significantly increased. With age, lesions develop centripetally, and gradually affect the whole cornea. Other symptoms appear subsequently, such as relapsed epithelial erosion, pannus fiber thickening, and deep stroma neovascularization. Non-specific epithelial abnormalities include atrophy, ectopia of the conjunctival goblet cells, and abnormalities of the basilar membrane. A scar matrix eventually forms, seriously affecting visual function.

Many studies of this syndrome have focused on the lens and the optic nerve, but very few have looked at the cornea<sup>[22-23]</sup>. There are several hypotheses about CAK pathogenesis. The first-proposed and currently widely accepted theory relates to deficiency of the corneal limbal stem cells<sup>[24-26]</sup>; other theories connect CAK to gelatinase B deficiency or hyperplasia of the conjunctival goblet cell. Glaucoma is another common complication for CAK patients, and high IOP resulted long-term corneal edema may be one of the factors leading to degeneration of the cornea<sup>[27]</sup>. In the current study, patients with CAK had an average central corneal thickness of 648  $\mu\text{m}$ , approximately 100  $\mu\text{m}$  thicker than in the control group. This indicates that the syndrome causes significantly increased thickness of the central cornea, which is consistent with the observations of others<sup>[28]</sup>. In the current study, patients with

CAK exhibited a high central corneal curvature, as well as significantly lower mean K and sim K and higher sim A compared with control participants. In addition, 66.7% of eyes from patients with CAK exhibited a flat cornea. Changes in corneal shape and thickness may be useful for enhancing our understanding of CAK. We also found that the majority of CAK patients exhibited relevant characteristics such as changes in shapes on the corneal height map and on the refractive power map of the front surface, and reduction of corneal curvature. Moreover, in designing this study, we prospectively selected a control group that matched the CAK group in sex and age, in order to reduce any confounding impact of sex, age, and other factors on corneal thickness. This also provided better conditions of morphological changes in the central cornea.

The shape of the central cornea is important for understanding its refractive index. In the current study, the majority of eyes in patients with CAK exhibited changes in their corneal thickness topology map and front surface refraction index map, as well as decreases in the corneal curvature. The thickness of the whole cornea was observed to be significantly greater in the eyes of CAK patients than in those of the control group. The central cornea remained the thinnest point, but the thickest corneal regions in CAK patients were the upper nasal, sub nasal, and central regions. In contrast, in the normal eye, the

cornea is thicker in the upper area than in the lower area. This trend was consistent with corneal performance in the CAK patients. Thickness measurements at nine corneal locations determined that 66.7% of eyes in our patient group had a flat cornea. In patients, the central and temporal corneal areas were the thinnest, while the thickest areas were in the nasal and superior regions. This may be due to glycosaminoglycan depositions in the scleral and corneal fibers, resulting in abnormal collagen or elastic fibers, or damage and thickening of the sclera and cornea. Since central corneal thickness can affect IOP, its measurement could help with diagnosing early-stage glaucoma in patients with progressive CAK. This study also found that morphological changes in the topographic map of refractive power in the anterior cornea were similar to the changes typical of high myopia<sup>[29]</sup>, suggesting that the corneal shape of patients with early CAK is similar to that of patients with high myopia. This tallies with the ocular manifestations that are known to be common in CAK patients.

In the current study, specular microscope examination showed normal corneal endothelial cell morphology and cell density; no corneal endothelial decomposition was detected, and we can therefore conclude that the increased thickness of the central cornea in patients with CAK is not caused by corneal endothelial cells. Edén *et al*<sup>[30]</sup> conducted confocal microscopy experiments on CAK patients, which revealed normal corneal epithelial cells and a thickened corneal substance layer. This suggests that the increased thickness of the central cornea in patients with CAK is due to the thickened corneal stromal layer.

Some studies of CAK patients have also found reduced tear secretion and ostial stenosis of the Meibomian gland<sup>[25]</sup>. In the present study, clinical examination findings in patients with early-stage CAK suggested Meibomian gland dysfunction or a pathologic lipid layer leading to tear film instability. It has been reported that BUT and SIT are highly correlated with age<sup>[31]</sup>. In this study, BUT and SIT were significantly decreased in patients with CAK. Central corneal changes also included increasing corneal thickness in patients with CAK. This might be due to the consistency of corneal and scleral tissue thickening caused by the *PAX6* gene mutation. In the current study, we did not find statistically significant differences in axial lengths between the CAK and healthy control groups, probably because of the young average age of our CAK patients, meaning that overall axial length changes were not obvious. This study has described the typical changes in corneal morphology and thickness in patients with early-stage CAK, which contributes to the understanding of CAK. However, the causes of these changes in corneal thickness and morphology require further study.

Although corneal epithelial changes such as inflammatory

and goblet cell invasion accompany conjunctivalization in the severe stages of CAK, in this study, dendritic cell invasion of wing and basal epithelial cell layers was observed at an early stage. In addition, the subbasal nerve density was pathologically high in the aniridic cornea *in vivo*. In a mouse model of CAK, no evidence of neurotrophic deficiency could be found in heterozygous *PAX6* corneas; however, the model differed developmentally from human patients and no corneal opacities were reported in the mice. IVCN assessment of the subbasal nerve plexus revealed a marked increase in nerve density in the central corneas of three patients compared with healthy human corneas assessed by the same laser-scanning IVCN technique. The most notable characteristics were prominent ridge structures between adjacent ridges at their base. Some or all of these structures were observed in healthy controls but, notably, the structures were present in an altered form in one patient with CAK. It is not known in what form the stem cell niche is present in congenital aniridia or whether it deteriorates over time; however, our findings indicate that this niche could exist morphologically to at least some degree in early CAK.

Since CAK inheritance is autosomal dominant and the incidence of pedigree progeny is 50%, it is important to conduct prenatal genetic testing. In addition to ocular abnormalities, CAK can also lead to complications including osseous abnormalities such as polydactyly and foot varus, dwarfism, auricle malformation, and genital abnormalities such as Wilms genitourinary tumors<sup>[32-34]</sup>. Those affected might not notice changes in their vision or inability to use the language to express symptom for infant, while afferent pupillary defects are undetectable. Rashid and Farhood<sup>[35]</sup> has hypothesized that the thickness of the central cornea can affect the measurement of IOP, and measuring the thickness of the central cornea can therefore help with the diagnosis of early glaucoma in CAK patients at high risk of progression.

In this study, our examination of transparent corneas in patients with early-stage CAK revealed subclinical epithelial inflammation and dense subbasal nerve degradation. The limitations of this study include its small sample size, bias associated with the single-center design, and possible selection bias in examining participants only from certain regions and only corneas tolerant to the imaging procedure. Future studies should examine a larger patient population (which exists in southern China), and report a longitudinal follow-up.

#### ACKNOWLEDGEMENTS

**Foundations:** Supported by the National Natural Science Foundation of China (No.81660158; No.81400372; No.81160118).

**Conflicts of Interest:** Du J, None; Liu RQ, None; Ye L, None; Li ZH, None; Zhao FT, None; Jiang N, None; Ye LH, None; Shao Y, None.

**REFERENCES**

- 1 Stahl ED. Anterior segment dysgenesis. *Int Ophthalmol Clin* 2014;54(3):95-104.
- 2 Tezcan B, Rich P, Bhide A. Prenatal diagnosis of WAGR syndrome. *Case Rep Obstet Gynecol* 2015;2015:928585.
- 3 He F, Liu DL, Chen MP, Liu L, Lu L, Ouyang M, Yang J, Gan R, Liu XY. A rare PAX6 mutation in a Chinese family with congenital aniridia. *Genet Mol Res* 2015;14(4):13328-13336.
- 4 McCulley TJ, Mayer K, Dahr SS, Simpson J, Holland EJ. Aniridia and optic nerve hypoplasia. *Eye (Lond)* 2005;19(7):762-764.
- 5 Ihnatko R, Eden U, Fagerholm P, Lagali N. Congenital aniridia and the ocular surface. *Ocul Surf* 2016;14(2):196-206.
- 6 Singh B, Mohamed A, Chaurasia S, Ramappa M, Mandal AK, Jalali S, Sangwan VS. Clinical manifestations of congenital aniridia. *J Pediatr Ophthalmol Strabismus* 2014;51(1):59-62.
- 7 Schneider S, Osher RH, Burk SE, Lutz TB, Montione R. Thinning of the anterior capsule associated with congenital aniridia. *J Cataract Refract Surg* 2003;29(3):523-525.
- 8 Lagali N, Edén U, Utheim TP, Chen X, Riise R, Dellby A, Fagerholm P. *In vivo* morphology of the limbal palisades of Vogt correlates with progressive stem cell deficiency in aniridia-related keratopathy. *Invest Ophthalmol Vis Sci* 2013;54(8):5333-5342.
- 9 Sakane Y, Yamaguchi M, Yokoi N, Uchino M, Dogru M, Oishi T, Ohashi Y, Ohashi Y. Development and validation of the Dry Eye-Related Quality-of-Life Score questionnaire. *JAMA Ophthalmol* 2013;131(10):1331-1338.
- 10 Hu PH, Gao GP, Yu Y, Pei CG, Zhou Q, Huang X, Zhang Y, Shao Y. Analysis of corneal topography in patients with pure microphthalmia in Eastern China. *J Int Med Res* 2015;43(6):834-840.
- 11 Liu QP, Zhang GB, Shao Y, Yi JL, Liu ZG, Tan YH, Chen W, Mao ZH, Wang L. The morphology and thickness of cornea in patients with Marfan syndrome. *Zhonghua Yan Ke Za Zhi* 2011;47(3):235-241.
- 12 Neuhaus C, Betz C, Bergmann C, Bolz HJ. Genetics of congenital aniridia. *Ophthalmologe* 2014;111(12):1157-1163.
- 13 Hingorani M, Hanson I, van Heyningen V. Aniridia. *Eur J Hum Genet* 2012;20(10):1011-1017.
- 14 Primignani P, Allegrini D, Manfredini E, Romitti L, Mauri L, Patrosso MC, Veniani E, Franzoni A, Longo AD, Gesu GP, Piozzi E, Damante G, Penco S. Screening of PAX6 gene in Italian congenital aniridia patients revealed four novel mutations. *Ophthalmic Genet* 2016;37(3):307-313.
- 15 Zhang X, Qin G, Chen G, Li T, Gao L, Huang L, Zhang Y, Ouyang K, Wang Y, Pang Y, Zeng B, Yu L. Variants in TRIM44 cause aniridia by impairing PAX6 expression. *Hum Mutat* 2015;36(12):1164-1167.
- 16 Kokotas H, Petersen MB. Clinical and molecular aspects of aniridia. *Clin Genet* 2010;77(5):409-420.
- 17 Shields RA, Cavuoto KM, McKeown CA, Chang TC. Unilateral foveal hypoplasia in a child with bilateral anterior segment dysgenesis. *Clin Case Rep* 2015;3(7):676-678.
- 18 Hou YN, Li S, Luan YX. Pax6 in collembola: adaptive evolution of eye regression. *Sci Rep* 2016;6:20800.
- 19 Azuma N, Nishina S, Yanagisawa H, Okuyama T, Yamada M. PAX6 missense mutation in isolated foveal hypoplasia. *Nat Genet* 1996;13(2):141-142.
- 20 Dobrowolski D, Orzechowska-Wylegala B, Wowra B, Wroblewska-Czajka E, Grolik M, Szczubialka K, Nowakowska M, Puzzolo D, Wylegala EA, Micali A, Aragona P. Cultivated oral mucosa epithelium in ocular surface reconstruction in aniridia patients. *Biomed Res Int* 2015;2015:281870.
- 21 Le Q, Deng SX, Xu J. *In vivo* confocal microscopy of congenital aniridia-associated keratopathy. *Eye (Lond)* 2013;27(6):763-766.
- 22 Khandgave TP, Kulkarni VN, Muzumdar DV, Puthran N. Bilateral optic nerve aplasia: a rare isolated central nervous system anomaly. *Middle East Afr J Ophthalmol* 2014;21(3):262-264.
- 23 Sasamoto Y, Hayashi R, Park SJ, Saito-Adachi M, Suzuki Y, Kawasaki S, Quantock AJ, Nakai K, Tsujikawa M, Nishida K. PAX6 isoforms, along with reprogramming factors, differentially regulate the induction of cornea-specific genes. *Sci Rep* 2016;6:20807.
- 24 Weissbart SB, Ayres BD. Management of aniridia and iris defects: an update on iris prosthesis options. *Curr Opin Ophthalmol* 2016;27(3):244-249.
- 25 Shiple D, Finklea B, Lauderdale JD, Netland PA. Keratopathy, cataract, and dry eye in a survey of aniridia subjects. *Clin Ophthalmol* 2015;9:291-295.
- 26 Holland EJ, Djalilian AR, Schwartz GS. Management of aniridic keratopathy with keratolimbal allograft: a limbal stem cell transplantation technique. *Ophthalmology* 2003;110(1):125-130.
- 27 Akagi T, Yoshikawa M, Nakanishi H, Yoshimura N. A case of WAGR syndrome in association with developmental glaucoma requiring bilateral Baerveldt glaucoma implants and subsequent tube repositioning. *Clin Ophthalmol* 2015;9:1081-1084.
- 28 Park SH, Park YG, Lee MY, Kim MS. Clinical features of Korean patients with congenital aniridia. *Korean J Ophthalmol* 2010;24(5):291-296.
- 29 Stulting RD, Fant BS; T-CAT Study Group. Results of topography-guided laser in situ keratomileusis custom ablation treatment with a refractive excimer laser. *J Cataract Refract Surg* 2016;42(1):11-18.
- 30 Edén U, Fagerholm P, Danyali R, Lagali N. Pathologic epithelial and anterior corneal nerve morphology in early-stage congenital aniridic keratopathy. *Ophthalmology* 2012;119(9):1803-1810.
- 31 Ozdemir M, Temizdemir H. Age- and gender-related tear function changes in normal population. *Eye (Lond)* 2010;24(1):79-83.
- 32 Ying M, Han R, Hao P, Wang L, Li N. Inherited KIF21A and PAX6 gene mutations in a boy with congenital fibrosis of extraocular muscles and aniridia. *BMC Med Genet* 2013;14:63.
- 33 Girgis N, Chen TC. Genetics of the pediatric glaucomas. *Int Ophthalmol Clin* 2011;51(3):107-117.
- 34 Janeczko M, Niedzielska E, Pietras W. Evaluation of renal function in pediatric patients after treatment for Wilms' tumor. *Adv Clin Exp Med* 2015;24(3):497-504.
- 35 Rashid RF, Farhood QK. Measurement of central corneal thickness by ultrasonic pachymeter and oculus pentacam in patients with well-controlled glaucoma: hospital-based comparative study. *Clin Ophthalmol* 2016;10:359-364.